Published in final edited form as:
J Neurophysiol. 2007 January ; 97(1): 858–870. doi:10.1152/jn.00884.2006.

Metabotropic Glutamate Receptors in the Main Olfactory Bulb Drive Granule Cell-Mediated Inhibition

Thomas Heinbockel[1], **Nora Laaris**[2], and **Matthew Ennis**[3]

[1]Department of Anatomy, Howard University College of Medicine, Washington, DC [2]Department of Pharmacology and Experimental Therapeutics, University of Maryland School of Medicine, Baltimore, Maryland [3]Department of Anatomy and Neurobiology, University of Tennessee Health Science Center, Memphis, Tennessee

Abstract

Main olfactory bulb (MOB) granule cells (GCs) express high levels of the group I metabotropic glutamate receptor (mGluR), mGluR5. We investigated the role of mGluRs in regulating GC activity in rodent MOB slices using whole cell patch-clamp electrophysiology. The group I/II mGluR agonist (±)-1-aminocyclopentane-*trans*-1,3-dicarboxylic acid (ACPD) or the selective group I agonist (RS)-3,5-dihydroxyphenylglycine (DHPG) depolarized (~20 mV) and increased the firing rate of GCs. In the presence of ionotropic glutamate and GABA receptor antagonists, DHPG evoked a more modest depolarization (~8 mV). In voltage clamp, DHPG, but not group II [(2S,2′R,3)-2-(2′,3′-dicarboxycyclopropyl) glycine, DCG-IV] or group III [L(+)-2-amino-4-phosphonobutyric acid, L-AP4] mGluR agonists, induced an inward current. The inward current reversed polarity near the potassium equilibrium potential, suggesting mediation by closure of potassium channels. The DHPG-evoked inward current was unaffected by the mGluR1 antagonist (*S*)-(+)-α-amino-4-carboxy-2-methylbenzeneacetic acid (LY367385), was blocked by the group I/II mGluR antagonist (α*S*)-α-amino-α-[(1*S*,2*S*)-2-carboxycyclopropyl]-9H-xanthine-9-propanoic acid (LY341495), and was absent in GCs from mGluR5 knockout mice. LY341495 also attenuated mitral cell-evoked voltage-sensitive dye signals in the external plexiform layer and mitral cell-evoked spikes in GCs. These results suggest that activation of mGluR5 increases GC excitability, an effect that should increase GC-mediated GABAergic inhibition of mitral cells. In support of this: DHPG increased the frequency of spontaneous GABAergic inhibitory postsynaptic currents in mitral cells and LY341495 attenuated the feedback GABAergic postsynaptic potential elicited by intracellular depolarization of mitral cells. Our results suggest that activation of mGluR5 participates in feedforward and/or feedback inhibition at mitral cell to GC dendrodendritic synapses, possibly to modulate lateral inhibition and contrast in the MOB.

INTRODUCTION

The main olfactory bulb (MOB) is the initial brain site that performs neural computations to decipher patterns of glomerular activity evoked by odors. Although our understanding of the roles of ionotropic glutamate receptors in the MOB circuitry has significantly improved over the last few years, relatively little is known about the function of metabotropic glutamate receptors (mGluRs). The eight mGluRs identified to date are subdivided into three groups

Address for reprint requests and other correspondence: T. Heinbockel, Dept. of Anatomy, Howard University College of Medicine, 520 W Street NW, Washington, DC 20059 (theinbockel@howard.edu)..

based on sequence homology, signal transduction mechanisms and pharmacology (Conn and Pin 1997): group I mGluRs (mGluR1, mGluR5), group II mGluRs (mGluR2, mGluR3), and group III mGluRs (mGluR4, mGluR6-8). Mitral and tufted cells, key output neurons in the MOB, express high levels of mGluR1, a group I mGluR (Martin et al. 1992; Masu et al. 1991; Shigemoto et al. 1992; van den Pol 1995). Recent studies demonstrate that mGluR1 plays a modest role in olfactory nerve (ON)-evoked excitation of mitral cells (De Saint Jan and Westbrook 2005; Ennis et al. 2006; Heinbockel et al. 2004; Yuan and Knöpfel 2006), including slow mitral cell oscillatory responses to ON input (Schoppa and Westbrook 2001; Yuan and Knöpfel 2006).

Comparatively less is known about the role(s) of mGluRs in regulating the excitability of GABAergic granule cells (GCs) in the MOB. GCs have been reported to express low to moderate levels of mGluR2 (group II) (Ohishi et al. 1993, 1998), and low levels of mGluR4 and mGluR7 (group III) (Kinzie et al. 1995; Ohishi et al. 1995; Saugstad 1997; Wada et al. 1998). GCs express the highest levels of mGluR5 (group I) in the brain (Romano et al. 1995). Electron microscopy studies demonstrate that mGluR5 is localized on portions of GC dendrites in the external plexiform layer (EPL) apposed to presynaptic glutamatergic synapses from mitral/tufted cell lateral dendrites (van den Pol 1995). This suggests that mGluR5 may mediate, at least in part, responses of GCs to glutamatergic inputs from mitral/tufted cells.

At present there is only limited information about the physiological actions and function of mGluRs on GCs. Studies in dissociated cultured rat and frog MOB neuronal preparations reported that activation of group I mGluRs with (±)-1-aminocyclopentane-*trans*-1,3-dicarboxylic acid (ACPD) or quisqualate increased Ca^{2+} release from internal stores in unidentified interneurons (Carlson et al. 1997; Geiling and Schild 1996). Activation of group II (mGluR2/3) receptors was also reported to inhibit high-voltage-activated Ca^{2+} currents in cultured frog olfactory bulb interneurons and to decrease spontaneous GABAergic inhibitory postsynaptic currents (IPSCs) in mitral/tufted cells (Bischofberger and Schild 1996). The function(s) of mGluRs on identified GCs in intact MOB preparations have not been investigated. Given the high level of expression of mGluR5s on GCs, we hypothesized that mGluRs would modulate GC excitability and responsiveness to glutamatergic synaptic input from mitral/tufted cells and, as a result, modulate GC-mediated GABAergic inhibition. To test these hypotheses, we studied the consequences of activation or blockade of mGluR5 on GCs using whole cell patch-clamp recordings and voltage-sensitive dye imaging in MOB slices from rats, wild-type mice, and mice with targeted gene deletions of group I mGluRs.

METHODS

Animals and genotyping

Animal experimentation and usage was in accordance with local Institutional Animal Care and Use Committee and the National Institutes of Health guidelines. Experimental animals were: commercially available male and female rats (Sprague-Dawley; Zivic Laboratories, Zelienople, PA) and wild-type mice (C57Bl/6J, Jackson Laboratory, Bar Harbor, ME) plus mGluR1 and mGluR5 mutant mice (C57Bl/6J background). The generation of mGluR1 and mGluR5 receptor knockout (KO) mice has been reported previously (Chiamulera et al. 2001; Conquet et al. 1994). Mutant mice were genotyped by polymerase chain reaction (PCR) of DNA from tail tip digests; homozygous mGluR1 mutant mice were also identified phenotypically by their progressive mobility deficit at several weeks of age (Conquet et al. 1994). For PCR genotyping, tail tips were digested at 56°C in 20 μl of proteinase K (1 μg/μl) in 48 mM Tris-HCl pH 8.0, 19 mM NaCl, 1.0 mM NaEDTA, 1.0% sodium dodecylsulfate until tips were completely dissolved (1–2 h). Sterile water (780 μl) was added to each digest and the samples heated at 95°C for 20 min to inactivate the proteinase K. Each PCR sample (25 μl) contained 1 μl of DNA digest in 1× PCR buffer, 1.5 mM $MgCl_2$, 0.2 mM each dTTP,

dCTP, dATP, dGTP and 0.625 Units of *Taq* polymerase. The oligonucleotide primers were 5 pmol/25 μl for lacZ, 10 pmol/25 μl for mGluR5 and 20 pmol/25 μl for neo. The thermocycler program was initiated by a 1 min denaturation step at 94°C followed by 39 amplification cycles: 94°C-1 min, 55°C-1 min, 72°C-1 min, and a final extension at 72°C for 10 min. The reaction products were separated by electrophoresis on 1.6% agarose gels and the amplicons visualized with ethidium bromide under UV illumination. The oligo-nucleotides for the neomycin resistance gene (mGluR1 and mGluR5 mutant mice) were 5′ GTGAATGAACTGCAGGACGA and 5′ ATACTTTCTCGGCAGGAGCA and generated a 170-bp amplicon. The oligonucleotides for lacZ (mGluR1 mutant mice) were 5′ CATCTACACCAACGTAACCTATCC and 5′ GATAACTGCCGTCACTCCAACGCAG and generated a 296-bp amplicon. To confirm that the mGluR5 mice were homozygous KO, they were also tested with oligonucleotides for the mGluR5 gene to ensure that no amplicon (442 bp) was generated. These oligonucleotides were 5′CACATGCCAGGTGACATCAT and 5′ CCATGCTGGTTGCAGAGTAA.

Slice preparation and electrophysiology

Juvenile (21- to 31-day-old) rats or mice were decapitated, and the MOBs were dissected out and immersed in artificial cerebrospinal fluid (ACSF, see following text) at 4°C as previously described (Heinbockel et al. 2004). Horizontal slices (400 μm thick) of the MOB were cut using a vibratome (Vibratome Series 1000, Ted Pella, Redding, CA). After 30 min at 30°C, slices were incubated in a holding bath at room temperature (22°C) until used. For recording, a single brain slice was placed in a perfusion bath recording chamber mounted on a microscope stage and maintained at 30 ± 0.5°C. Slices were submerged in ACSF (composition in the following text) flowing at 2.5 to 3 ml/min.

Visually guided recordings were obtained from GCs in the GC layer and mitral cells in the mitral cell layer with near-infra red differential interference contrast (NIR DIC) optics, water-immersion objectives and a BX50WI microscope (Olympus Optical, Tokyo) (Stuart et al. 1993). NIR transillumination was at 900 nm (filter transmission, 850–950 nm) concentric with the objective and optimized for DIC. A 0.25-in CCD camera (CCD 100, Dage, Stamford, CT), fitted with a 3-to-1 zooming coupler (Optem, Fairport, NY) was used. Contrast was enhanced in real-time using an image processor (Model 794, Hughes Aircraft, Carlsbad, CA), and the image was displayed on a monochrome monitor (Dage HR120, Dage-MTI, Michigan City, IN).

Recording pipettes were pulled on a Flaming-Brown P-97 puller (Sutter Instrument, Novato, CA) from standard-wall filamented 1.5-mm diameter borosilicate glass; tip diameter was 2–3 μm, tip resistance was 5–8 MΩ. Seal resistance was routinely >1GΩ. Liquid junction potential was 9–10 mV; reported voltage measurements were not corrected for this potential. Data were obtained using an Axopatch 200B amplifier (Axon Instruments, Foster City, CA). Analog signals were recorded, low-pass Bessel filtered at 2 kHz, and digitized on videotape (AR Vetter, Rebersburg, PA) and computer disk (Axoscope/Clampex, Axon Instruments). Data were also collected through a Digidata-1200A (Axopatch) or Digidata 1322A (Multiclamp) Interface (Axon Instruments) and digitized at 10 kHz. Holding currents were generated under manual control by the recording amplifier. Spontaneous inhibitory postsynaptic currents (IPSCs, Fig. 6) were analyzed over 1-min epochs using Mini Analysis Program (version 6.0.1. Synaptosoft, Decatur, GA). The detection threshold for IPSCs was 20 pA. In current clamp, membrane resistance was calculated from the amount of steady-state current required to hyperpolarize the cell by 10 mV, typically from –70 to –80 mV. In voltage clamp, membrane resistance was calculated from currents elicited by negative voltage pulses (10 mV, 1 s, 0.05 Hz). Current versus voltage (*I-V*) plots were obtained over potentials from –130 to –40 mV (see Fig. 5*B*, *inset*) using a voltage step protocol (10-mV step intervals, 500 ms/step, V_{hold} = –70 mV) in the

presence of synaptic blockers [2-amino-5-phosphonovaleric acid (APV), 6-cyano-7-nitroquinoxalene-2,3-dione (CNQX), gabazine] and TTX. Numerical data are expressed as the means ± SE. Unless otherwise noted, tests for statistical significance ($P < 0.05$) were performed using Student's *t*-test.

Optical imaging voltage-sensitive dye signals

Optical imaging of voltage-sensitive dye signals was used to investigate activity patterns evoked by stimulation of the lateral olfactory tract (LOT, see following text). Slices were harvested as described in the preceding text. After incubation at room temperature in ACSF, slices were stained with the voltage-sensitive dye RH-414 (100 μM; Molecular Probes, Eugene, OR). The dye was dissolved in ACSF, and a single slice was placed in a static bath containing this solution, continuously aerated with 95% O_2-5% CO_2 for 30–45 min. The stained slice was then transferred to an immersion-type recording chamber, and continuously perfused at 2 ml/min with ACSF at room temperature. To washout unbound dye, stained slices were perfused with ACSF for ≥15 min before initiating the optical recording. Methods used for recording voltage-sensitive optical signals are similar to those described in detail elsewhere (Keller et al. 1998; Laaris et al. 2006). The recording chamber was mounted on a fixed stage upright microscope (Olympus BX50WI), rigidly mounted on a vibration-isolation table. A stabilized D.C. power source was used to power a 100 W tungsten-halogen lamp, and the light from this lamp was band-limited with interference (540 ± 30 nm band-pass, Omega Optical, Brattleboro, VT) and heat filters. Light from the preparation was collected through a ×10 water-immersion objective (Olympus), and projected onto a hexagonal 464 element array of photodiodes (NeuroPlex, OptImaging, Fairfield, CT). Each photodiode sampled optical signals from a region of ~60 × 60 μm^2. The current output from each photodiode was separately converted to voltages, and amplified in two separate stages (×1,000), multiplexed, and digitized at 12-bit resolution with an A/D converter. Optical signals were filtered at 500 Hz before digitizing. Data were collected and stored on a personal computer controlled by NeuroPlex software (OptImaging). Optical signals were collected at a sampling rate of 1.63 kHz. Optical responses were averaged for five consecutive stimulation trials, collected at 20-s intervals. To correct for spatial differences in illumination intensity and light path length, the signal recorded from each detector was divided by the resting light intensity calculated for the corresponding detector. The resting light intensity for each detector was calculated by subtracting the intensity values recorded while the shutter was closed from those recorded while the shutter was open when no stimulation was applied. The resulting signal amplitudes are expressed as a fractional change in fluorescence, relative to baseline fluorescence levels ($\Delta F/F_0$). To quantify the relative changes in light fluorescence, we calculated the mean and SE of the $\Delta F/F_0$ during the 50 ms preceding the stimulus. For statistical analyses, the LOT-evoked response amplitudes are expressed as the means ± SE above these mean baseline values. To illustrate the spatial distribution of optical signals (Fig. 7), poststimulus signal amplitudes were color-coded and interpolated as a percentage of the prestimulus signal amplitude. Analyses of data were performed on an Apple Macintosh computer, using routines developed in Igor (WaveMetrics, Lake Oswego, OR). To precisely identify the regions in the slice from which optical recordings were collected, a custom-designed beam splitting device (Microscope Services, Rockville, MD) was used to simultaneously project the images of the slice and light from light-emitting diodes embedded in the photodiode array onto the image plane of a CCD camera (Dage CCD72, Michigan City, IN). This allowed us to correlate voltage-sensitive dye optical signals with the laminar borders of different layers in MOB slices (see Fig. 7).

In addition to voltage-sensitive dye-related signals, optical responses may also arise from sources intrinsic to the slice (Grinvald et al. 1988; Yuste et al. 1997). To determine if such intrinsic signals contributed to the waveforms recorded in our study, we performed experiments in slices that were not stained with the voltage-sensitive dyes ($n = 2$); no optical signals were

detected in these control experiments using methods identical to those for recording voltage-sensitive dye signals. We also tested the dependence of these signals on the illumination wavelength. When the illumination was changed to a wavelength outside the absorption spectrum of the dye (≥800 nm), no optical signal was detected in the MOB. This suggests that the optical signals represent dye-related responses and are not the result of intrinsic optical signals. Dye-related optical signals may also originate from activation of glial cells. In this case, the optical responses recorded from glial cells are expected to exhibit a slow time course (>1 s) compared with that of neuronal responses (Konnerth et al. 1987). In the mouse MOB, glomerular layer astrocytes exhibit long-lasting (~1 s) responses to single ON shocks (De Saint Jan and Westbrook 2005). However, the evoked optical signals recorded in the MOB had only a single depolarizing component, whose duration was <85 ms. Additionally, previous studies demonstrate that glial toxins do not alter voltage-sensitive dye optical signals in MOB evoked by ON stimulation (Keller et al. 1998). Taken together, these findings suggest that the dye-related optical signals analyzed in the present study reflect neuronal responses, and are not related to signals originating from glial cells.

Stimulation of the glomerular layer and LOT

The glomerular layer (GL) or the LOT were electrically stimulated to directly activate mitral cells, and in turn, mitral to granule cell glutamatergic synapses as previously reported (Aroniadou-Anderjaska et al. 2000; Egger et al. 2005; Halabisky et al. 2000; Schoppa and Westbrook 1999; Schoppa et al. 1998). Focal stimulation was achieved with a bipolar electrode constructed from a pair of twisted stainless-steel wires (50 μm), insulated except for bluntly cut tips. Stimuli were isolated monophasic square wave pulses (10–100 μA in amplitude, 0.1 ms in duration) delivered by a Grass S8800 stimulator (Astro-Med, West Warwick, RI) and an isolated constant current source (Grass PSIU6, Astro-Med).

Drugs and solution

The standard ACSF consisted of (in mM): 120 NaCl, 3 KCl, 1.3 $CaCl_2$, 1.3 $MgSO_4$, 10 glucose, 25 $NaHCO_3$, and 5 BES [*N*,*N*-bis(2-hydroxyethyl)-2-aminoethanesulfonic acid] 5% O_2-5% CO_2-saturated, pH 7.27, 300 mOsm (Heyward et al. 2001). The standard pipette-filling solution consisted of (in mM) 125 K gluconate, 2 $MgCl_2$, 10 HEPES, 2 Mg_2ATP, 0.2 Na_3GTP, 1 NaCl, and 0.2 EGTA. To record inhibitory postsynaptic currents (IPSCs) in mitral cells, a high-Cl^- pipette solution was used to shift the chloride equilibrium potential close to 0 mV, thus reversing the polarity of IPSCs; this solution consisted of (in mM) 55 KCl, 75 K_2SO_4, 7 NaCl, 1 $MgSO_4$, 10 HEPES, 2 MgATP, 2 Mg_2ATP, and 0.2 Na_3GTP and 200 μM BAPTA. Recording medium and pipette solution components were from Sigma-Aldrich (St. Louis, MO). The following drugs were bath applied: ACPD, D-2-amino-5-phosphonopentanoic acid (APV), 6-cyano-7-nitroquinoxaline-2-3-dione (CNQX), (2S,2′R,3)-2-(2′,3′-dicarboxycyclopropyl) glycine (DCG-IV), (RS)-3,5-dihydroxyphenylglycine (DHPG), (2-(3-carboxypropyl)-3-amino-6-(4 methoxyphenyl)-pyridazinium bromide (gabazine, SR-95531), L(+)-2-amino-4-phosphonobutyric acid (L-AP4), (α*S*)-α-amino-α-[(1*S*,2*S*)-2-carboxycyclopropyl]-9H-xanthine-9-propanoic acid (LY341495), (*S*)-(+)-α-amino-4-carboxy-2-methylbenzeneacetic acid (LY367385), tetraethylammonium chloride (TEA), and tetrodotoxin (TTX). All drugs were supplied by Tocris (Ellisville, MO), except for gabazine, TEA chloride, and TTX (Sigma-Aldrich, St. Louis, MO).

RESULTS

GCs were identified visually with NIR-DIC by their relatively small soma size, location in the GC layer, and high-input resistance (rats: 560.6 ± 55.2 MΩ, n = 10; mice: 947.5 ± 106.2 MΩ, n = 46). We recorded from 26 GCs in rat and 135 GCs in mouse MOB slices. All 15 cells

recorded in the granule cell layer and filled with biocytin were confirmed to be GCs by subsequent histological examination (data not shown).

Group I/II mGluR agonist depolarizes granule cells and increases their firing rate

We first investigated the actions of the group I/II mGluR agonist, ACPD, on GC membrane potential and spontaneous spike generation in current-clamp recording mode. As shown in Fig. 1, bath application of ACPD (50 μM) strongly depolarized all GCs tested (n = 24); such depolarization was often accompanied by increased action potential firing rate (15/24 cells tested) and increased frequency of EPSPs. The depolarizing effect of ACPD on GCs was similar in rats and wild-type mice [peak membrane depolarization compared with baseline (ΔmV) in rats = 19.1 ± 2.7 mV, n = 14; ΔmV in mice = 22.7 ± 3.9 mV, n = 10; P = 0.088, Fig. 1*F*). Prolonged application (>2 min) of ACPD resulted in spike broadening, decreased spike amplitude and gradual reduction in firing of GCs (i.e., depolarization block; Fig. 1*B*). All of these effects were fully reversible during washout.

To determine if the preceding effects were mediated by direct activation of mGluRs on GCs, ACPD was applied in the presence of blockers of ionotropic glutamate and $GABA_A$ receptors ("synaptic blockers"): CNQX (10 μM), APV (50 μM), and gabazine (5 μM). As shown in Fig. 1*C*, the synaptic blockers reduced GC spontaneous synaptic activity (e.g., compare baseline in Fig. 1, *A* vs. *C* and *D* vs. *E*; see also Fig. 4), including EPSPs as well as spontaneous action potentials, without significantly changing the resting membrane potential (ΔmV in synaptic blockers: 0.2 ± 0.3 mV, n = 30). In the presence of synaptic blockers (Fig. 1*C*), the depolarizing action of ACPD persisted although it was reduced in amplitude (ΔmV = 8.4 ± 1.9 mV, n = 9) compared with control ACSF (ΔmV = 19.1 ± 2.7 mV, P = 0.018, independent t-test). Similarly, in wild-type mice (Fig. 1*F*) ACPD evoked a smaller depolarization in the presence of synaptic blockers (ΔmV = 5.5 ± 0.6 mV, n = 11) compared with control conditions (ΔmV = 22.7 ± 3.9 mV; P = 0.00018, independent t-test). The peak depolarization evoked by ACPD in synaptic blockers was not significantly different between rats and mice (P = 0.088, Fig. 1*F*). ACPD, and DHPG (see following text), were recently demonstrated to strongly and directly depolarize mitral cells and increase their firing rate via activation of mGluR1 (Heinbockel et al. 2004). We interpret the reduced effect of ACPD and DHPG in the presence of synaptic blockers as follows. ACPD applied in normal media directly depolarizes granule cells and also indirectly excites them as a consequence of increased glutamate release from mitral cells. The latter effect is eliminated when ACPD is applied in the presence of synaptic blockers.

Effects essentially identical to those of ACPD were obtained with the selective group I agonist DHPG (50 μM; Figs. 1, *D* and *E*, and 4*C*). DHPG depolarized (ΔmV in mice = 15.3 ± 3.2 mV) and increased the firing rate of all GCs tested (n = 10). As with the effect of ACPD, the action of DHPG persisted but was reduced in amplitude in the presence of synaptic blockers (ΔmV in synaptic blockers: 8.0 ± 1.1 mV, n = 11; P = 0.032, independent t-test, Figs. 1*E* and 4*C*). The peak membrane depolarization produced by ACPD in normal media or synaptic blockers did not differ significantly from the values produced by DHPG in similar conditions (ACPD vs. DHPG, normal ACSF: P = 0.16; ACPD vs. DHPG with synaptic blockers: P = 0.059).

Selective group I mGluR agonists activate GCs

GCs express both group I and II receptor subtypes (Ohishi et al. 1993, 1998; Romano et al. 1995; van den Pol 1995). Group I mGluRs include the mGluR1 and mGluR5 subtypes. Therefore several potential mGluR subtypes could mediate the effects of broad-spectrum agonists. To further investigate the specific mGluRs involved in responses to ACPD and DHPG, we explored the actions of preferential agonists for the three mGluR groups. In voltage-clamp recordings (V_{hold} = –70 mV), DHPG (50 μM) applied in normal ACSF elicited an inward current and an increase in the frequency of spontaneous EPSCs (Fig. 2*A*). As noted above, the

increased EPSC frequency is probably due to activation of mitral cells and subsequent glutamate release, which acted on ionotropic glutamate receptors on GCs. Consistent with this, synaptic blockers eliminated sEPSCs and consequently the DHPG-evoked increase in sEPSCs. In the presence of synaptic blockers, neither the group III agonist L-AP4 (100 μM, Fig. 2*B*) nor the group II agonist DCG-IV (20 μM, Fig. 2*C*) elicited significant currents ($P = 0.17$ and $P = 0.53$, respectively, $n = 8$). The lack of effect of DCG-IV and L-AP4 is not due to insufficient concentration as both were applied well above their respective EC50s (<1 μM) for group II and III mGluRs, respectively, and at concentrations known to activate these receptors in olfactory bulb neurons (Schoppa and Westbrook 1997; Trombley and Westbrook 1990, 1992). By contrast, in the same GCs, the group I agonist DHPG (50 μM) elicited an inward current (8.0 ± 0.8 pA, $n = 24$; $P = 0.00001$; Fig. 2*E*).

GCs express high levels of mGluR5, but mGluR1 is not present in GCs or is expressed at very low levels (van den Pol 1995). This suggests that the effects of DHPG are probably mediated via activation of mGluR5 on GCs. The specificity of DHPG was further assessed with mGluR antagonists. We first tested the effects of LY367385, a selective mGluR1 antagonist with negligible actions on group II and III mGluRs, and effects on mGluR5 only at a concentration in excess of 100 μM (Clark et al. 1997; Salt et al. 1999). Application of LY367385 (10–100 μM) in the presence of synaptic blockers did not elicit any measurable currents in GCs (Δ pA: 0.4 ± 0.2 pA, $n = 5$, $P = 0.18$). In the presence of synaptic blockers, LY367385 did not affect the amplitude of the inward current elicited by DHPG compared with DHPG applied alone in synaptic blockers (Fig. 3) [ΔpA DHPG = 8.0 ± 0.8 pA, $n = 24$ (see preceding text) vs. ΔpA DHPG + LY367385 = 6.8 ± 3.1 pA, $n = 4$; $P = 0.59$, independent *t*-test]. The failure of LY367385 to decrease the inward current indicates that it does not involve postsynaptic mGluR1 on GCs and further that DHPG-evoked glutamate release from mitral/tufted cells (via activation of mGluR1 in the presence of fast synaptic blockers) does not itself lead to a detectable mGluR5-mediated current in GCs. The lack of effect of LY367385 is not attributable to an insufficient concentration for mGluR1 blockade as recent experiments (Heinbockel et al. 2004) demonstrated that an identical LY367385 concentration completely antagonized the effects of DHPG at mGluR1 in mitral cells. As shown in Fig. 3, application of LY341495 (100 μM), which blocks all mGluRs at this concentration (Fitzjohn et al. 1998; Kingston et al. 1998), completely blocked DHPG responses in GCs (ΔpA in DHPG + LY341495: 0.6 ± 0.3 pA, $n = 6$; $P = 0.001$, independent *t*-test).

DHPG excitation of granule cells is present in mGluR1 knockout mice and absent in mGluR5 knockout mice

The preceding pharmacological results suggest that the effect of DHPG on GCs is mediated by activation of mGluR5. We took advantage of mice with targeted deletions of the mGluR5 or mGluR1 genes (Chiamulera et al. 2001; Conquet et al. 1994) to further investigate the role of these receptor subtypes on GCs. GCs recorded in slices harvested from wild-type and mGluR5$^{-/-}$ mice were similar in terms of basic electrophysiological properties, such as resting membrane potential (–65.8 ± 0.9 mV, $n = 82$, wild-type vs. –69.9 ± 2.3 mV, $n = 15$, mGluR5$^{-/-}$ mice, $P = 0.07$), input resistance: (947.5 ± 106.2 MΩ, $n = 46$, wild-type vs. 861.5 ± 86.5 MΩ, $n = 15$, mGluR5$^{-/-}$ mice, $P = 0.68$) and ability to generate spikes (95.2%, $n = 63$, wild-type vs. 100%, $n = 15$, mGluR5$^{-/-}$ mice). In mGluR5$^{-/-}$ mice, DHPG applied in normal media depolarized and increased the firing of GCs (Fig. 4, *A*, *left*, and *C;* ΔmV = 17.4 ± 4.6 mV, $n = 7$, $P = 0.009$), similar to the effects of DHPG in wild-type mice (Figs. 1*D* and 4*C*; ΔmV = 15.3 ± 3.2 mV). There was no difference between the DHPG-evoked depolarization in wild-type and mGluR5$^{-/-}$ mice ($P = 0.7$). Thus as in wild-type mice, the effect of DHPG on GCs in mGluR5 knockout animals is mediated as a consequence of mGluR1-mediated excitation of mitral cells, followed by activation of ionotropic glutamate receptors on GCs. In agreement with this, DHPG had no discernible effects on GCs in slices from mGluR5$^{-/-}$ mice

when applied in the presence of synaptic blockers (Fig. 4*A*, *right*; Δ mV = 0.6 ± 0.4 mV, n = 7, P = 0.23), and the response was therefore significantly less than that in mGluR5$^{-/-}$ mice in normal media (P = 0.003).

The effects of DHPG were also tested on GCs in slices harvested from mGluR1 knockout mice. Because mGluR1s are absent in these mice (Conquet et al. 1994; Heinbockel et al. 2004), DHPG should excite GCs solely via activation of postsynaptic mGluR5, and this excitation should persist in the presence of synaptic blockers. In agreement with this, DHPG elicited a comparable depolarization of GCs from mGluR1$^{-/-}$ mice in normal media (ΔmV: 6.0 ± 0.8 mV, n = 4; P = 0.005) and in the presence of synaptic blockers (ΔmV: 8.8 ± 2.0 mV, n = 9; P = 0.002); there was no significant difference between the amplitude of the DHPG-evoked depolarization in normal media and in synaptic blockers (P = 0.39, independent *t*-test). The response of GCs from mGluR1$^{-/-}$ mice in normal media was smaller than that in GCs from wild-type in normal media (P = 0.02, independent *t*-test). The amplitude of the DHPG-evoked depolarization in synaptic blockers was nearly identical in wild-type (8.0 ± 1.1 mV, data from preceding text) and mGluR1$^{-/-}$ mice (8.8 ± 2.0 mV; P = 0.73, independent *t*-test). These data provide further evidence that the DHPG-evoked depolarization depends on postsynaptic activation of mGluR5 on GCs and also that DHPG-evoked excitation of mitral/tufted cells (via mGluR1) does not release sufficient glutamate to induce an mGluR5-mediated depolarization of GCs. However, we cannot exclude the possibility that DHPG, via mGluR5, might cause the release of other excitatory transmitters from neuronal elements presynaptic to GCs.

DHPG elicits an inward current in granule cells

The preceding experiments demonstrate that the effects of DHPG on GCs persist in the presence of synaptic blockers and therefore appear to be directly mediated. DHPG was also tested in the presence of TTX (1 μM) to further preclude presynaptic actions. The magnitude of the DHPG-evoked current was unaffected by TTX (8.0 ± 0.8 pA, n = 24, synaptic blockers vs. 8.2 ± 0.9 pA, n = 10, synaptic blockers + TTX; P = 0.88). This indicates that the DHPG-evoked current in GCs does not involve TTX-sensitive sodium channels or spike-dependent transmitter release from neuronal elements presynaptic to GCs. The current-voltage (*I-V*) relationship of the DHPG-evoked inward current in GCs was investigated at potentials from –130 to –40 mV using voltage step protocols (see METHODS) in the presence of synaptic blockers [CNQX (10 μM), APV (50 μM), gabazine (5 μM)] and TTX (1 μM) in the bathing solution. The *I-V* relationship of the DHPG current was nearly linear between –140 and –70 mV, and reversed in polarity at approximately –100 mV (Fig. 5, *A* and *B*). The inward current appeared to decrease slightly at potentials positive to –60 mV, suggesting that it may involve multiple components; DHPG-evoked currents at membrane potential positive to –40 mV were not explored.

The reversal potential of the DHPG current (approximately –100 mV) is nearly identical to the estimated K^+ equilibrium potential (–96 mV), suggesting that the current may be mediated, at least in part, by closure of K^+ channels. In agreement with this, DHPG application significantly increased the membrane input resistance of GCs (synaptic blockers + TTX: 682.9 ± 65.5 MΩ; synaptic blockers + TTX + DHPG: 884.3 ± 89.4 MΩ, n = 10, P < 0.0001). The specific involvement of K^+ ions was further assessed with bath-applied K^+ channel blockers: $BaCl_2$ (300 μM), 4-aminopyridine (100 μM), TEA (20 mM), CsCl (5 mM). K^+ channels were blocked by bath-applied reagents rather than including them in the recording pipette as the later method is insufficient to completely block K^+ channels in mitral cells (Heinbockel et al. 2004). *I-V* curves generated with K^+ channel blockers in the bath before and after DHPG (50 μM) application revealed that DHPG evoked no significant current at membrane potentials negative to –60 mV (Fig. 5, *C* and *D*); a small but significant inward current was present at –60 to –40 mV. DHPG did not significantly alter the input resistance of GCs in the presence of K^+ channel blockers (K^+ channel blockers: 1,900.8 ± 167.9 MΩ; K^+ channel blockers + DHPG: 1,882.9

± 183.0 MΩ, $n = 17$, $P = 0.93$). Taken together, these results indicate that a major component of the DHPG-evoked inward current at the membrane potentials tested is due to closure of K^+ channels.

Activation of mGluR5 increases GABAergic inhibition of mitral cells

Excitatory mGluR5s on GCs may function, in part, to facilitate feedback and feedforward inhibition of mitral cells. Is mGluR5-evoked excitation of GCs sufficient to increase GABA release onto mitral cells? To address this question, we first used voltage-clamp recordings to determine if DHPG-evoked activation of GCs alters GABAergic inhibitory input to mitral cells. A high concentration of chloride was used in the patch pipette to increase the detectibility of IPSCs; under these conditions IPSCs appeared as inward currents (see METHODS). In the presence of ionotropic glutamate receptor blockers, DHPG (50 μM) increased the frequency of IPSCs in mitral cells in wild-type mice from 1.8 ± 0.4 to 10.3 ± 2.8 Hz ($P = 0.0025$, $n = 8$; Fig. 6, *A* and *C*). However, the increase in IPSCs was accompanied by a large inward current (–106.4 ± 10.4 pA) in mitral cells, mediated by direct activation of mGluR1 as previously reported (Heinbockel et al. 2004). To preclude the latter effect, similar experiments were performed in mGluR1$^{-/-}$ mice. DHPG, applied in the presence of ionotropic glutamate receptor blockers, increased the frequency of IPSCs from 4.3 ± 1.4 to 16.3 ± 3.0 Hz ($P = 0.004$, $n = 6$) but did not elicit a significant inward current in mitral cells (Fig. 6*B*). In all experiments, IPSCs were abolished by the $GABA_A$ receptor antagonist gabazine (Fig. 6, *A* and *B*). The frequency of IPSCs in wild-type versus mGluR1$^{-/-}$ mice was not significantly different in control conditions ($P = 0.078$) and during DHPG application ($P = 0.11$).

Blockade of mGluRs reduces mitral cell-evoked excitation of GCs

The findings in the preceding text demonstrate that pharmacological activation of mGluR5 on GCs increases GABAergic inhibition of mitral cells. Does activation of mGluR5 play a functional role in GC responses to glutamatergic synaptic input from mitral cells and are these receptors involved in GC-mediated feedback inhibition of mitral cells? To address these questions, we first assessed the effects of the mGluR antagonist LY341495 on GC responses to mitral cell input using optical imaging of voltage-sensitive dyes. As recently reported (Laaris et al. 2006), single shocks applied to the LOT elicited optical responses that were first observed in the external plexiform layer (EPL; 7.3 ± 0.4 ms onset latency, $n = 10$; Fig. 7). LOT-evoked responses then spread sequentially into the superficial GCL. LOT-evoked responses were abolished by removal of Ca^{2+} from the ACSF, by application of TTX (0.5 μM) or CNQX-APV, indicating that they are postsynaptically mediated (Laaris et al. 2006). As shown in Fig. 7, application of LY341495 (100 μM) reduced the peak amplitude of the LOT-evoked voltage-sensitive dye signal in the EPL by 48.8 ± 3.1% (range, 34.9–53.7%; $n = 5$ slices, $P = 0.0002$).

The preceding findings suggest that mGluR blockade reduces GC excitability to mitral/tufted cell synaptic input. To further investigate this, current-clamp recordings were used to asses the effects of mGluR blockade on GC responses to mitral/tufted cell input. As shown in Fig. 8*A*, single shocks applied to the glomerular layer to directly activate mitral cells elicited spikes in GCs as previously reported (Schoppa et al. 1998). LY341495 reversibly reduced the mean response probability to mitral/tufted cell input, i.e., the occurrence of a spike, from 79.8 ± 3.7% to 49.5 ± 8.3% (Fig. 8, *A* and *B; n* = 10 cells, $P = 0.009$). Although LY341495 produced a small, nonsignificant mean hyperpolarization of the resting membrane potential (–0.5 ± 0.6 mV; control: –55.7 ± 2.8, LY341495: –56.2 ± 3.0 mV; $n = 10$ cells, $P = 0.4$; Fig. 8*C*), a cell-by-cell analysis revealed that the reduction of evoked-spiking by LY341495 varied with the degree of hyperpolarization. As shown in Fig. 8*D*, the response probability to mitral/tufted cell input decreased with increasing hyperpolarization ($r = –0.73$; $P = 0.01$, $n = 10$). Additionally, LY341495 significantly hyperpolarized the six cells that exhibited the largest reduction in evoked spiking (Fig. 8*D*; –1.8 ± 0.2 mV, control: –54.9 ± 0.2 mV, LY341495: –56.7 ± 0.1 mV;

$P = 0.017$); spike threshold was not significantly affected by LY341495 in these cells (–46.0 ± 3.4 vs. –46.9 ± 4.2 mV; $P = 0.42$). LY341495 produced a small, but nonsignificant reduction in the amplitude of evoked EPSPs (control: 9.7 ± 0.6 mV, LY341495: 9.0 + 0.6 mV; $n = 10$ cells, $P = 0.08$; Fig. 8*E*), and there was no consistent relationship between the EPSP amplitude and the degree of hyperpolarization ($r = –0.29$; $P = 0.4$; $n = 10$). In parallel voltage-clamp recordings (Fig. 8, *F* and *G*), LY341495 did not significantly affect the amplitude, onset latency, kinetics or integral of the glomerular-evoked EPSC in GCs ($n = 10$; amplitude: 15.6 ± 3.3 vs. 15.2 ± 3.3 pA, $P = 0.7$; onset latency: 6.1 ± 2.1 vs. 4.8 ± 0.9 ms, $P = 0.3$; 10–90% rise time: 37.4 ± 14.3 vs. 41.7 ± 18.9 ms, $P = 0.5$; half-width: 145.9 ± 30.8 vs. 145.8 ± 30.9 ms, $P = 0.9$). Taken together, these findings suggest that the reduction of evoked spiking in GCs by LY341495 was not due to presynaptic modulation of glutamate release from mitral/tufted cell dendrites but may be due to the degree of GC hyperpolarization.

Blockade of mGluRs reduces feedback inhibition of mitral cells. The preceding experiments indicate that inactivation of mGluRs significantly attenuates mitral cell-evoked excitation of GCs. Does blockade of mGluRs decrease GC-mediated inhibition of mitral cells? To address this question, we determined if LY341495 alters feedback IPSPs elicited by direct depolarization of individual mitral cells. As previously reported (Isaacson and Strowbridge 1998), depolarizing current steps applied to mitral cells in the presence of TTX and TEA were followed by a feedback IPSP (Fig. 9). Bath application of LY341495 (100 μM) reduced the peak amplitude of the feedback IPSP from –5.9 ± 0.4 to –3.9 ± 0.5 mV ($P < 0.001$, $n = 5$). The integral of the feedback IPSP was reduced by nearly 60% ($P < 0.000001$, $n = 5$). The frequency of spontaneous IPSPs was reduced from 1.1 ± 0.1 to 0.6 ± 0.1 IPSPs/s after addition of LY341495 ($P < 0.000001$, $n = 5$, data not shown). The $GABA_A$ receptor antagonist gabazine further reduced the integral of the IPSP compared with LY341495 ($P < 0.000001$). Gabazine practically eliminated spontaneous IPSPs (0.01 ± 0.001 IPSPs/s, $P < 0.000001$). These results demonstrate that blockade of mGluRs reduces GC-mediated feedback inhibition of mitral cells.

DISCUSSION

The present study demonstrates that activation and inactivation of mGluR5 directly increase and decrease, respectively, the excitability of GABAergic GCs in the MOB. Our results indicate that mGluR5 modulates the strength of GC responses to glutamatergic inputs from mitral/tufted cells and GC-mediated dendrodendritic feedback inhibition in the MOB. These findings suggest that activation of mGluR5 by glutamate released from mitral/tufted cells amplifies lateral inhibition and therefore may increase contrast in the MOB network.

Activation of mGluR5 directly depolarizes GCs

In normal media, ACPD and DHPG robustly depolarized (~20 mV) and increased the firing rate of GCs. These effects were due mediated by direct activation of mGluR5 on GCs and indirect excitation (i.e., increased glutamate release) due to activation of mGluR1 on mitral cells. In the presence of synaptic blockers, the depolarizing response to the mGluR agonists persisted, although it was reduced in amplitude (6–8 mV). The latter result indicates that ACPD and DHPG directly depolarize GCs. In all cases, identical effects of ACPD and DHPG were observed in slices harvested from rats and wild-type mice.

ACPD and DHPG activate the two known group I receptor subtypes, mGluR1 and mGluR5. Several results indicate that the direct actions of these agonists on GCs are mediated exclusively via activation of mGluR5. First, the selective mGluR1 antagonist LY367385 did not block the effect of DHPG on GCs, whereas it completely eliminates DHPG-evoked, mGluR1-mediated excitation of mitral cells at identical concentrations (Heinbockel et al. 2004). Second, DHPG had no discernible effects on GCs in mGluR5 knockout mice, whereas it readily activated GCs in mGluR1 knockout mice. Third, neither group II nor group III mGluR agonists elicited

currents in GCs. However, because the effects of group II/III agonists were only studied at a single holding potential (–70 mV), we do not exclude the possibility that these agonists may have effects on voltage-gated currents in GCs inoperative at the membrane potential tested.

Activation of mGluR5 induces an inward current in GCs

DHPG elicited an inward current in voltage clamp recordings of mouse GCs. The *I-V* relationship of the DHPG current in GCs was nearly linear between –140 and –70 mV and reversed in polarity at approximately –100 mV. The current appeared to decrease at potentials positive to –60 mV, suggesting that it may involve multiple components similar to DHPG currents in several brain areas (see Anwyl 1999 for review). The identity of the current present at more positive potentials remains to be determined but may involve voltage-gated Ca^{2+} channels, Ca^{2+}-dependent nonselective cation conductances (Congar et al. 1997; Crepel et al. 1994; Guerineau et al. 1995; Raggenbass et al. 1997) or electrogenic Na^{+}/Ca^{2+} exchangers (Keele et al. 1997; Lee and Boden 1997; Staub et al. 1992). A major component of the inward current appears to be mediated by closure of K^{+} channels as it was abolished by K^{+} channel blockers. This is further supported by the observation that DHPG increased the membrane input resistance of GCs in normal ACSF but did not alter it in the presence of K^{+} channel blockers. Previous studies demonstrate GCs have a prominent A-like K^{+} current, I_A (Schoppa and Westbrook 1999). A reduction of I_A is unlikely to fully account for the DHPG-evoked inward current as I_A in GCs is sharply voltage dependent, activates at potentials positive to –45 mV, and inactivates rapidly (Schoppa and Westbrook 1999). By contrast, the DHPG-evoked current varied linearly with voltages negative to –45 mV, and its steady state amplitude was measured at a time point several hundred milliseconds after inactivation of I_A. Given their similar properties (e.g., linear *I-V* relationship), a reasonable mechanism for the DHPG-evoked current is a decrease in a leak K^{+} current. In agreement with this possibility, activation of group I mGluRs has been reported to reduce leak K^{+} currents (Glaum and Miller 1992; Guerineau et al. 1994; McCormick and von Krosigk 1992; Takeshita et al. 1996).

Activation of mGluR5 on GCs increases GABA release from GCs

The present results demonstrate that activation of mGluR5 on GCs increases GABAergic inhibition of mitral cells. In the presence of ionotropic glutamate receptor antagonists, DHPG increased the frequency of GABAergic IPSCs in mitral cells. Such effects persisted in mGluR1 knockout mice, indicating that direct activation of mGluR5 is sufficient to drive GABA release from GCs. These findings suggest that the DHPG-evoked closure of K^{+} channels provides sufficient depolarization to increase GABA release from GCs.

Pharmacological activation of mGluR5 increases GABA release from GCs, but does mGluR5 modulate GABA release in response to synaptic input from mitral/tufted cells? The present findings suggest that mGluR5 plays an important modulatory role in regulating GABA release from GCs after activation of mitral/tufted cells. Inactivation of mGluRs with LY341495 significantly reduced the magnitude of voltage-sensitive dye signals in the EPL elicited by mitral/tufted cell activation. We have previously shown that such signals primarily reflect glutamatergic excitation of GC dendrites (Laaris et al. 2006). LY341495 also reduced spiking responses elicited by antidromic stimulation of mitral/tufted cells. Although we cannot ascribe these effects solely to blockade of mGluR5, these result suggests that activation of mGluRs by endogenously released glutamate tonically modulates the excitability of GCs. LY341495 reduced evoked responses in the voltage-sensitive dye experiments to a greater extent than in the whole cell patch-clamping experiments. One possibility is that mGluR5 components of the evoked response in normal media may degrade in whole cell recordings because the intracellular components involved in mGluR5 transduction could run-down as a result of dialysis. This in turn would lead to a reduced effect of LY341495 in the whole cell recordings compared with the voltage-sensitive dye recordings.

Consistent with the reduction of mitral/tufted cell-evoked excitation of GCs, application of LY341495 significantly reduced the feedback IPSP evoked by intracellular depolarization of individual mitral cells. These effects do not appear to be mediated by presynaptic suppression of glutamate release as LY341495 did not reduce the mitral/tufted cell-evoked EPSP or EPSC in GCs. The reduction in mitral/tufted-evoked spiking and the feedback IPSP may to be due to the small tonic hyperpolarization in some GCs elicited by LY341495, which would bias the GC away from spike threshold and reduce evoked spiking. The present findings show that activation of mGluR5 depolarizes GCs, at least in part, via K^+ channel closure. Inactivation of mGluR5 by LY341495 may prevent ambient or mitral/tufted cell-evoked, glutamate from closing K^+ channels, accounting for the observed hyperpolarization. It is less clear how this would influence the feedback IPSP. K^+ channel blockers have been reported to increase (Schoppa and Westbrook 1999) or have no effect (Halabisky et al. 2000) on the dendrodendritically mediated feedback IPSP in mitral cells. An additional possibility is that LY341495 prevents glutamate-evoked, mGluR-mediated Ca^{2+} release from internal stores in GCs (Carlson et al. 1997; Geiling and Schild 1996), leading to reduced GABA release, or that it alters other aspects of GC excitability. Additional studies are needed to address these possibilities.

Functional considerations

mGluR5 is localized on portions of GC dendrites in the external plexiform layer directly opposed to presynaptic glutamatergic synapses from mitral/tufted cell lateral dendrites (van den Pol 1995). Our results suggest that activation of mGluR5 increases mitral/tufted cell-evoked excitation of GCs and, in turn, facilitates dendrodendritic GABA release onto mitral/tufted cells. GC-mediated lateral inhibition plays an important role in odor contrast enhancement in the MOB (Yokoi et al. 1995). mGluR-mediated responses typically have a slow time course and are maximally activated by high-frequency stimulation (for review, see Anwyl 1999). Activation of mGluR5 on GCs may function to enhance the temporal envelope of lateral inhibition beyond that mediated by ionotropic glutamate receptors or to amplify lateral inhibition during repetitive sensory input associated with high-frequency investigative sniffing.

Acknowledgments

We thank Dr. F. L. Margolis and F. Scipio for genotyping mGluR knockout mice.

GRANTS

This work was supported in part by the Whitehall Foundation, Howard University New Faculty Research Program, and National Institutes of Health Grants 2-S06-GM-08016-36, DC-03195, and DC-00347.

REFERENCES

Anwyl R. Metabotropic glutamate receptors: electrophysiological properties and role in plasticity. Brain Res Rev 1999;29:83–120. [PubMed: 9974152]

Aroniadou-Anderjaska V, Zhou F-M, Priest CA, Ennis M, Shipley MT. Tonic and synaptically evoked presynaptic inhibition of sensory input to the rat olfactory bulb via $GABA_B$ heteroreceptors. J Neurophysiol 2000;84:1194–1203. [PubMed: 10979995]

Bardoni R, Puopolo M, Magherini PC, Belluzzi O. Potassium currents in periglomerular cells of frog olfactory bulb in vitro. Neurosci Lett 1996;210:95–98. [PubMed: 8783281]

Bandrowski AE, Huguenard JR, Prince DA. Baseline glutamate levels affect group I and II mGluRs in layer V pyramidal neurons of rat sensorimotor cortex. J Neurophysiol 2003;89:1308–1316. [PubMed: 12626613]

Bischofberger J, Schild D. Glutamate and N-acetylaspartylglutmate block HVA calcium currents in frog olfactory bulb interneurons via an mGluR2/3-like receptor. J Neurophysiol 1996;76:2089–2093. [PubMed: 8890318]

Carlson GC, Slawecki ML, Lancaster E, Keller A. Distribution and activation of intracellular Ca^{2+} stores in cultured olfactory bulb neurons. J Neurophysiol 1997;78:2176–2185. [PubMed: 9325384]

Chiamulera C, Epping-Jordan MP, Zocchi A, Marcon C, Cottiny C, Tacconi S, Corsi M, Orzi F, Conquet F. Reinforcing and locomotor stimulant effects of cocaine are absent in mGluR5 null mutant mice. Nat Neurosci 2001;4:873–874. [PubMed: 11528416]

Clark BP, Baker SR, Goldsworthy J, Harris JR, Kingston AE. 2-Methyl-4-carboxyphenylglycine (LY367385) selectively antagonizes metabotropic glutamate mGluR1 receptors. Bioorg Med Chem Lett 1997;7:2777–2870.

Congar P, Leinekugel X, Ben-Ari Y, Crepel V. A long-lasting calcium-activated nonselective cationic current is generated by synaptic stimulation or exogenous activation of group I metabotropic glutamate receptors in CA1 pyramidal neurons. J Neurosci 1997;17:5366–5379. [PubMed: 9204921]

Conn PJ, Pin JP. Pharmacology and functions of metabotropic glutamate receptors. Annu Rev Pharmacol Toxicol 1997;37:205–237. [PubMed: 9131252]

Conquet F, Bashir ZI, Davies CH, Daniel H, Ferraguti F, Bordi F, Franz-Bacon K, Reggiani A, Matarese V, Condé F, Collingridge GL, Crépel F. Motor deficit and impairment of synaptic plasticity in mice lacking mGluR1. Nature 1994;372:237–243. [PubMed: 7969468]

Crepel V, Aniksztejn L, Ben-Ari Y, Hammond C. Glutamate metabotropic receptors increase a Ca^{2+}-activated nonspecific cationic current in CA1 hippocampal neurons. J Neurophysiol 1994;72:1561–1569. [PubMed: 7823086]

De Saint Jan D, Westbrook GL. Detecting activity in olfactory bulb glomeruli with astrocyte recording. J Neurosci 2005;25:2917–2924. [PubMed: 15772351]

Egger V, Svoboda K, Mainen ZF. Dendrodendritic synaptic signals in olfactory bulb granule cells: local spine boost and global low-threshold spike. J Neurosci 2005;25:3521–3530. [PubMed: 15814782]

Ennis M, Zhu M, Heinbockel T, Hayar A. Olfactory nerve-evoked, metabotropic glutamate receptor-mediated synaptic responses in rat olfactory bulb mitral cells. J Neurophysiol 2006;95:2233–2241. [PubMed: 16394070]

Fitzjohn SM, Bortolotto ZA, Palmer MJ, Doherty AJ, Ornstein PL, Schoepp DD, Kingston AE, Lodge D, Collingridge GL. The potent mGlu receptor antagonist LY341495 identifies roles for both cloned and novel mGlu receptors in hippocampal synaptic plasticity. Neuropharmacology 1998;37:1445–1458. [PubMed: 9886667]

Friedman D, Strowbridge BW. Functional role of NMDA autoreceptors in olfactory mitral cells. J Neurophysiol 2000;84:39–50. [PubMed: 10899181]

Geiling H, Schild D. Glutamate-mediated release of Ca^{2+} in mitral cells of the olfactory bulb. J Neurophysiol 1996;76:563–570. [PubMed: 8836244]

Glaum SR, Miller RJ. Metabotropic glutamate receptors mediate excitatory transmission in the nucleus of the solitary tract. J Neurosci 1992;12:2251–2258. [PubMed: 1351539]

Grinvald A, Frostig RD, Lieke E, Hildesheim R. Optical imaging of neuronal activity. Physiol Rev 1998;68:1285–1366. [PubMed: 3054949]

Guerineau NC, Bossu JL, Gähwiler BH, Gerber U. Activation of a nonselective cationic conductance by metabotropic glutamatergic and muscarinic agonist in CA3 pyramidal neurons of the rat hippocampus. J Neurosci 1995;15:4395–4407. [PubMed: 7790916]

Guerineau NC, Gähwiler BH, Gerber U. Reduction of resting K^+ current by metabotropic glutamate and muscarinic receptors in rat CA3 cells: mediation by G-proteins. J Physiol 1994;474:27–33. [PubMed: 8014895]

Halabisky B, Friedman D, Radojicic M, Strowbridge BW. Calcium influx through NMDA receptors directly evokes GABA release in olfactory bulb granule cells. J Neurosci 2000;20:5124–34. [PubMed: 10864969]

Heinbockel T, Heyward PM, Conquet F, Ennis M. Regulation of main olfactory bulb mitral cell excitability by metabotropic glutamate receptor mGluR1. J Neurophysiol 2004;92:3085–3096. [PubMed: 15212418]

Heyward P, Ennis M, Keller A, Shipley MT. Membrane bistability in olfactory bulb mitral cells. J Neurosci 2001;21:5311–5320. [PubMed: 11438607]

Isaacson JS, Strowbridge BW. Olfactory reciprocal synapses: dendritic signaling in the CNS. Neuron 1998;20:749–761. [PubMed: 9581766]

Keele NB, Arvanov VL, Shinnick-Gallagher P. Quisqualate-preferring metabotropic glutamate receptor activates Na^{+}-Ca^{2+} exchange in rat baso-lateral amygdala neurons. J Physiol 1997;499:87–104. [PubMed: 9061642]

Keller A, Yagodin S, Aroniadou-Anderjaska A, Zimmer LA, Ennis M, Sheppard NF, Shipley MT. Functional organization of rat olfactory bulb glomeruli revealed by optical imaging. J Neurosci 1998;18:2602–2612. [PubMed: 9502819]

Kingston AE, Ornstein PL, Wright RA, Johnson BG, Mayne NG, Burnett JP, Belagaje R, Wu S, Schoepp DD. LY341495 is a nanomolar potent and selective antagonist of group II metabotropic glutamate receptors. Neuropharmacology 1998;37:1–12. [PubMed: 9680254]

Kinzie JM, Saugstad JA, Westbrook GL, Segerson TP. Distribution of metabotropic glutamate receptor 7 messenger RNA in the developing and adult rat brain. Neuroscience 1995;69:167–176. [PubMed: 8637615]

Konnerth A, Obaid AL, Salzberg DM. Optical recording of electrical activity from parallel fibers and other cell types in skate cerebellar slices in vitro. J Physiol 1987;393:681–702. [PubMed: 3446807]

Laaris N, Carlson GC, Keller A. Thalamic-evoked synaptic interactions in barrel cortex revealed by optical imaging. J Neurosci 2000;20:1529–1537. [PubMed: 10662842]

Laaris N, Puche A, Ennis M. Complementary postsynaptic activity patterns elicited in olfactory bulb by stimulation of mitral/tufted and centrifugal fiber inputs to granule cells. J Neurophysiol 2007;97:296–306. [PubMed: 17035366]

Lee K, Boden PR. Characterization of the inward current induced by metabotropic glutamate receptor stimulation in rat ventromedial hypothalamic neurones. J Physiol 1997;504.3:649–663. [PubMed: 9401972]

Martin LJ, Blackstone CD, Huganir RL, Price DL. Cellular localization of a metabotropic glutamate receptor in rat brain. Neuron 1992;9:259–270. [PubMed: 1323311]

Masu M, Tanabe Y, Tsuchida K, Shigemoto R, Nakanishi S. Sequence and expression of a metabotropic glutamate receptor. Nature 1991;349:760–765. [PubMed: 1847995]

McCormick DA, von Krosigk M. Corticothalamic activation modulates thalamic firing through glutamate "metabotropic" receptors. Proc Natl Acad Sci USA 1992;89:2774–2778. [PubMed: 1313567]

Ohishi H, Akazawa C, Shigemoto R, Nakanishi S, Mizuno N. Distributions of the mRNAs for L-2-amino-4-phosphobutyrate-sensitive metabotropic glutamate receptors, mGluR4 and mGluR7, in the rat brain. J Comp Neurol 1995;360:555–570. [PubMed: 8801249]

Ohishi H, Neki A, Mizuno N. Distribution of a metabotropic glutamate receptor, mGluR2, in the central nervous system of the rat and mouse: an immunohistochemical study with a monoclonal antibody. Neurosci Res 1998;30:65–82. [PubMed: 9572581]

Ohishi H, Shigemoto R, Nakanishi S, Mizuno N. Distribution of the mRNA for a metabotropic glutamate receptor, mGluR2, in the central nervous system of the rat. Neuroscience 1993;53:1009–1018. [PubMed: 8389425]

Petralia RS, Wang YX, Singh S, Wu C, Shi L, Wei J, Wenthold RJ. A monoclonal antibody shows discrete cellular and subcellular localizations of mGluR1 alpha metabotropic glutamate receptors. J Chem Neuroanat 1997;13:77–93. [PubMed: 9285353]

Pin J-P, Duvoisin R. Neurotransmitter receptors I. The metabotropic gluta-mate receptors: structure and functions. Neuropharmacology 1995;34:1–26. [PubMed: 7623957]

Raggenbass M, Pierson P, Metzger D, Alberi S. Action of a metabotropic glutamate receptor agonist in rat lateral septum: induction of a sodium-dependent inward aftercurrent. Brain Res 1997;776:75–87. [PubMed: 9439798]

Redman S. Quantal analysis of synaptic potential in neurons of the central nervous system. Physiol Rev 1990;70:165–198. [PubMed: 2404288]

Rivadulla C, Martinez LM, Varela C, Cudeiro J. Completing the corticofugal loop: a visual role for the corticogeniculate type 1 metabotropic glutamate receptor. J Neurosci 2002;22:2956–2962. [PubMed: 11923460]

Romano C, Sesma MA, McDonald CT, O'Malley K, van den Pol AN, Olney JW. Distribution of metabotropic glutamate receptor mGluR5 immunoreactivity in rat brain. J Comp Neurol 1995;355:455–469. [PubMed: 7636025]

Sahara Y, Kubota T, Ichikawa M. Cellular localization of metabotropic glutamate receptors mGluR1, 2/3, 5 and 7 in the main and accessory olfactory bulb of the rat. Neurosci Lett 2001;312:59–62. [PubMed: 11595334]

Salin PA, Lledo PM, Vincent JD, Charpak S. Dendritic glutamate autoreceptors modulate signal processing in rat mitral cells. J Neurophysiol 2001;85:1275–1282. [PubMed: 11247996]

Salt TE, Turner JP, Kingston AE. Evaluation of agonists and antagonists acting at group I metabotropic glutamate receptors in the thalamus in vivo. Neuropharmacology 1999;38:1505–1510. [PubMed: 10530812]

Saugstad JA, Kinzie JM, Shinohara MM, Segerson TP, Westbrook GL. Cloning and expression of rat metabotropic glutamate receptor 8 reveals a distinct pharmacological profile. Mol Pharmacol 1997;51:119–125. [PubMed: 9016353]

Schoepp DD, Jane DE, Monn JA. Pharmacological agents acting at subtypes of metabotropic glutamate receptors. Neuropharmacology 1999;38:1431–1476. [PubMed: 10530808]

Schoppa NE, Kinzie JM, Sahara Y, Segerson TP, Westbrook GL. Dendrodendritic inhibition in the olfactory bulb is driven by NMDA receptors. J Neurosci 1998;18:6790–6802. [PubMed: 9712650]

Schoppa NE, Westbrook GL. Modulation of mEPSCs in olfactory bulb mitral cells by metabotropic glutamate receptors. J Neurophysiol 1997;78:1468–1475. [PubMed: 9310436]

Schoppa NE, Westbrook GL. Regulation of synaptic timing in the olfactory bulb by an A-type potassium current. Nat Neurosci 1999;2:1106–13. [PubMed: 10570488]

Schoppa NE, Westbrook GL. Glomerulus-specific synchronization of mitral cells in the olfactory bulb. Neuron 2001;31:639–651. [PubMed: 11545722]

Shigemoto R, Nakanishi S, Mizuno N. Distribution of the mRNA for a metabotropic glutamate receptor (mGluR1) in the central nervous system: an in situ hybridization study in adult and developing rat. J Comp Neurol 1992;322:121–135. [PubMed: 1430307]

Smith TC, Jahr CE. Self-inhibition of olfactory bulb neurons. Nat Neurosci 2002;5:760–766. [PubMed: 12089528]

Spors H, Grinvald A. Spatio-temporal dynamics of odor representations in the mammalian olfactory bulb. Neuron 2002;34:301–315. [PubMed: 11970871]

Staub C, Vranesic I, Knöpfel T. Responses to metabotropic glutamate receptor activation in cerebellar purkinje cells: induction of an inward current. Eur J Neurosci 1992;4:832–839. [PubMed: 12106306]

Stuart GJ, Dodt HU, Sakmann B. Patch-clamp recordings from the soma and dendrites of neurons in brain slices using infrared video microscopy. Pfluegers 1993;423:511–518.

Takeshita Y, Harata N, Akaike N. Suppression of K^+ conductance by metabotropic glutamate receptor in acutely dissociated large cholinergic neurons of rat caudate putamen. J Neurophysiol 1996;76:1545–1558. [PubMed: 8890274]

Trombley PQ, Westbrook GL. Excitatory synaptic transmission in cultures of rat olfactory bulb. J Neurophysiol 1990;64:598–606. [PubMed: 1976766]

Trombley PQ, Westbrook GL. L-AP4 inhibits calcium currents and synaptic transmission via a G-protein-coupled glutamate receptor. J Neurosci 1992;12:2043–2050. [PubMed: 1318954]

van den Pol A. Presynaptic metabotropic glutamate receptors in adult and developing neurons: autoexcitation in the olfactory bulb. J Comp Neurol 1995:253–271. [PubMed: 7499528]

Wada E, Shigemoto R, Kinoshita A, Ohishi H, Mizuno N. Metabotropic glutamate receptor subtypes in axon terminals of projection fibers from the main and accessory olfactory bulbs: a light and electron microscopic immunohistochemical study in the rat. J Comp Neurol 1998;393:493–504. [PubMed: 9550154]

Watanabe K, Kawana E. Selective retrograde transport of tritiated D-aspartate from the olfactory bulb to the anterior olfactory nucleus, pyriform cortex and nucleus of the lateral olfactory tract in the rat. Brain Res 1984;296:148–151. [PubMed: 6201233]

Yokoi M, Mori K, Nakanishi S. Refinement of odor molecule tuning by dendrodendritic synaptic inhibition in the olfactory bulb. Proc Natl Acad Sci USA 1995;92:3371–3375. [PubMed: 7724568]

Yuan Q, Knöpfel T. Olfactory nerve stimulation-evoked mGluR1 slow potentials, oscillations and calcium signaling in mouse olfactory bulb mitral cells. J Neurophysiol 2006;95:3097–3104. [PubMed: 16467433]

Yuste R, Tank DW, Kleinfeld D. Functional study of the rat cortical microcircuitry with voltage-sensitive dye imaging of neocortical slices. Cereb Cortex 1997;7:546–558. [PubMed: 9276179]

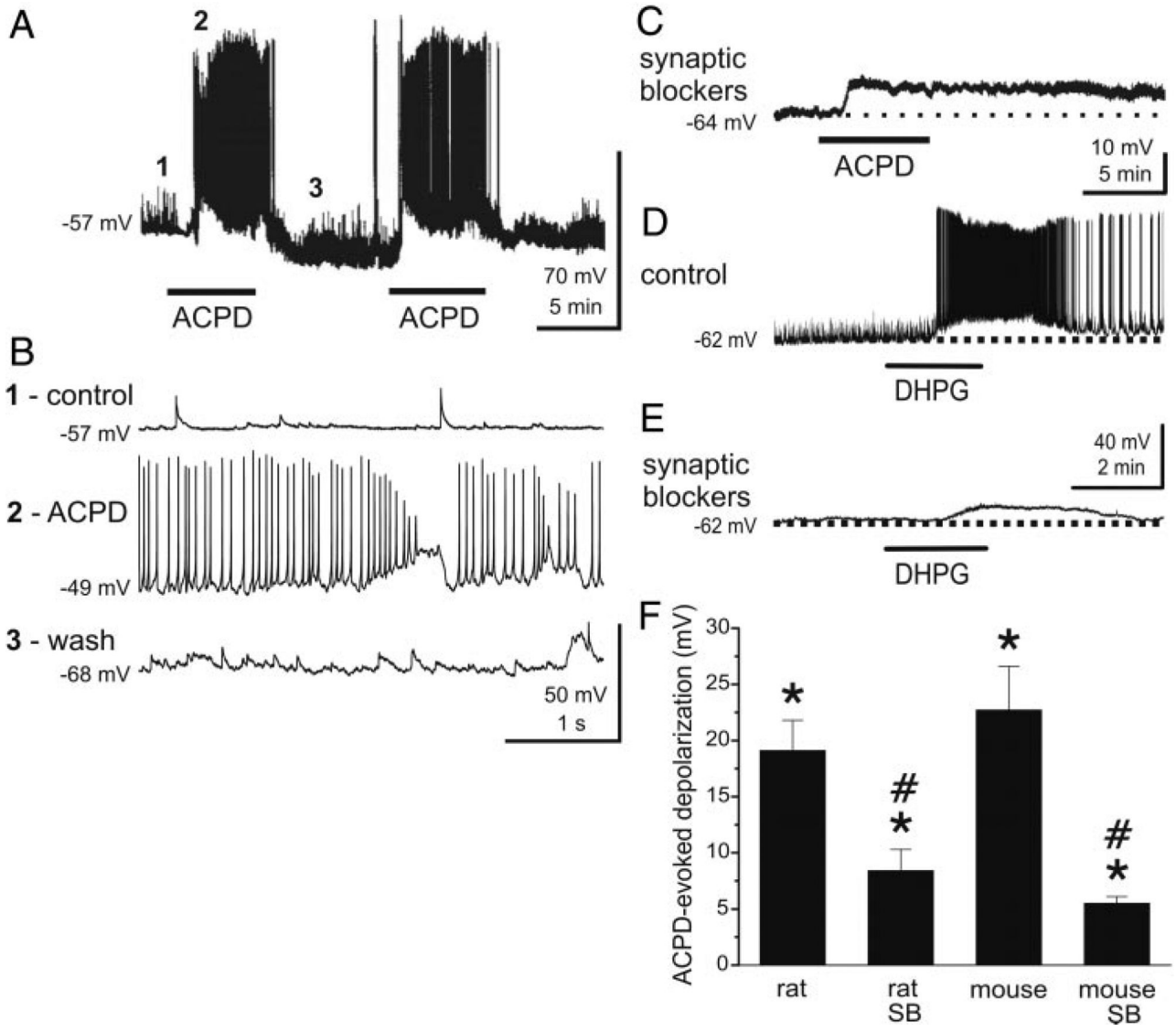

Fig. 1.

Group I and group I/II mGluR agonists directly excite granule cells (GCs). *A*: bath application of the group I/II mGluR agonist (±)-1-aminocyclopentane-*trans*-1,3-dicarboxylic acid (ACPD; 50 μM, at lower bars) resulted in membrane potential depolarization and increased action potential firing in this rat GC. Similar responses were produced by re-application of ACPD, indicating minimal desensitization to the agonist. ACPD-evoked responses were reversible, and the membrane potential typically returned to control levels within 5 min after washout. *B*: response of the cell in *A* is shown at an extended time scale. Traces 1–3 correspond to the similarly labeled time points in *A*. *C*: application of blockers of fast synaptic transmission [synaptic blockers; 6-cyano-7-nitroquinoxalene-2,3-dione (CNQX), 10 μM; 2-amino-5-phosphonovaleric acid (APV), 50 μM; gabazine, 5 μM] to the same cell shown in *A* reduced the baseline spontaneous synaptic activity. The depolarizing response to ACPD under these conditions was smaller than that without synaptic blockers and did not reach spike threshold. *D*: group I mGluR agonist (RS)-3,5-dihydroxyphenylglycine (DHPG; 50 μM) depolarized and increased the firing rate of this typical mouse GC. *E*: in the same cell shown in *D*, blockers of fast synaptic transmission reduced baseline spontaneous synaptic activity [spontaneous excitatory postsynaptic potentials (EPSPs)] and DHPG evoked a more moderate

depolarization. *F*: bar graph summarizing the effects of ACPD on rat and mouse GCs with or without synaptic blockers (SB). Data are expressed as changes in membrane voltage compared with control; see text for numbers of GCs tested. DHPG group data are included in Fig. 4. *, significantly different from control, $P < 0.05$, paired *t*-test. #, significantly different from non-SB group, $P < 0.05$, independent *t*-test, see text for specific *P* values.

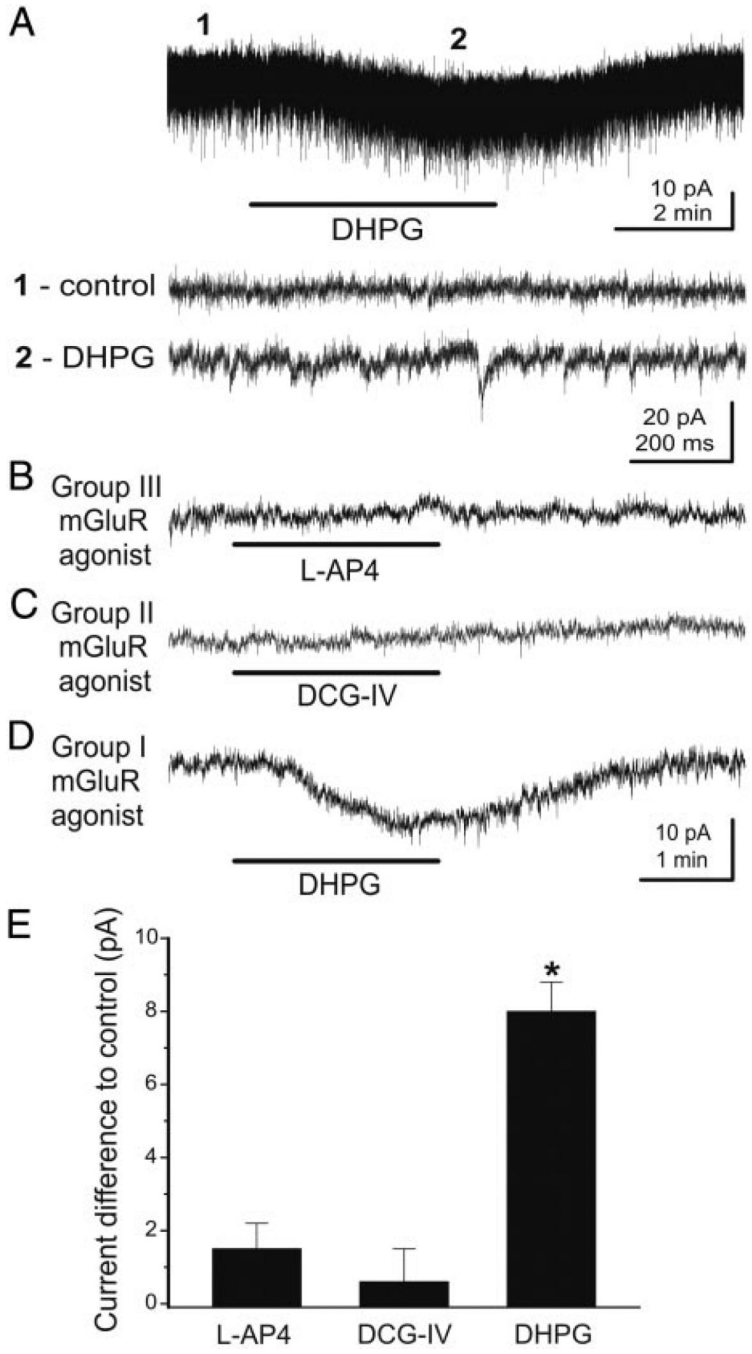

Fig. 2.

Group I, but not group II or III, mGluR agonists activate GCs. *A*:in voltage-clamp recordings (V_{hold} = –70 mV) from this rat GC, DHPG (50 μM) applied in normal media evoked an inward current and an increase in the frequency of spontaneous excitatory postsynaptic currents (EPSCs). Recordings at time points 1 and 2 are illustrated in the corresponding lower tracers at a faster time scale. Note increase in the frequency of EPSCs during DHPG application. Experiments in *B*–*E* were performed in the presence of synaptic blockers in mouse GCs: CNQX (10 μM), APV (50 μM) and gabazine (5 μM). *B* and *C*: application of the group III agonist L (+)-2-amino-4-phosphonobutyric acid (L-AP4; 100 μM) or the group II agonist (2S,2′R,3)-2-(2′,3′-dicarboxycyclopropyl)glycine (DCG-IV; 20 μM) did not alter the membrane current.

D: by contrast, the selective group I agonist DHPG (50 μM) produced a significant inward current in the presence of synaptic blockers. Recordings in *B–D* are from the same cell; $V_{hold} = -70$ mV. *E*: bar graph summarizing the effects the mGluR agonists tested in the presence of synaptic blockers; data are expressed as changes in membrane current compared with control (synaptic blocker only condition); see text for numbers of GCs tested. *, significantly different from control, $P < 0.05$, paired *t*-test.

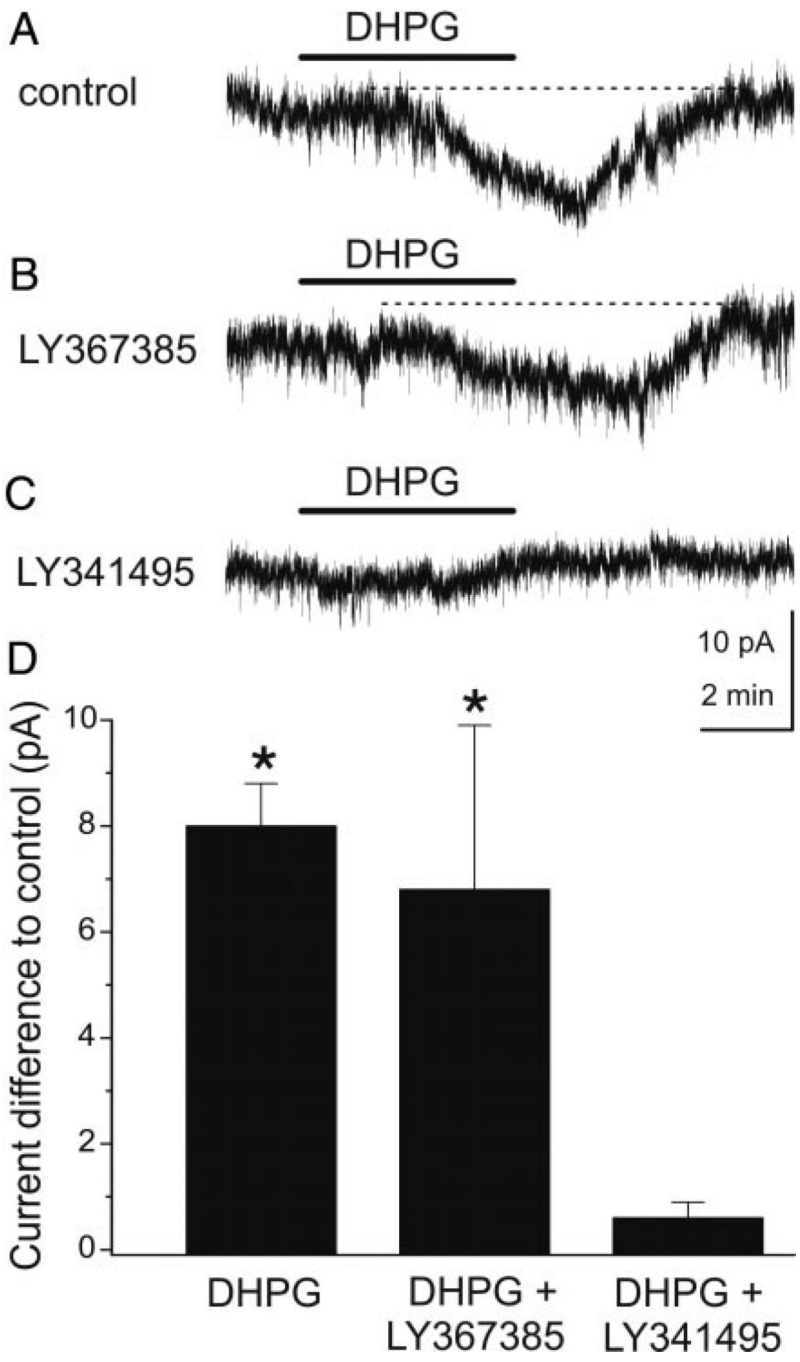

Fig. 3.

Effects of mGluR antagonists on GC responses to DHPG. *A* and *B*: inward current evoked by DHPG (*A*) in this mouse GC was not attenuated by the selective mGluR1 antagonist (*S*)-(+)-α-amino-4-carboxy-2-methylbenzeneacetic acid (LY367385; 100 μM), as shown in (*B*); V_{hold} = –70 mV in all panels. *C*: nonselective mGluR antagonist (α*S*)-α-amino-α-[(1*S*,2*S*)-2-carboxycyclopropyl]-9H-xanthine-9-propanoic acid (LY341495; 100 μM) blocked the DHPG-evoked inward current in the same cell, suggesting that the group I receptor mGluR5 mediates the response to DHPG. All experiments were performed in the presence of synaptic blockers: CNQX (10 μM), APV (50 μM), and gabazine (5 μM). *D*: bar graph summary of group data; data are expressed as changes in membrane current compared with control in synaptic blockers;

see text for numbers of GCs tested. *, significantly different from control, $P < 0.05$, paired *t*-test.

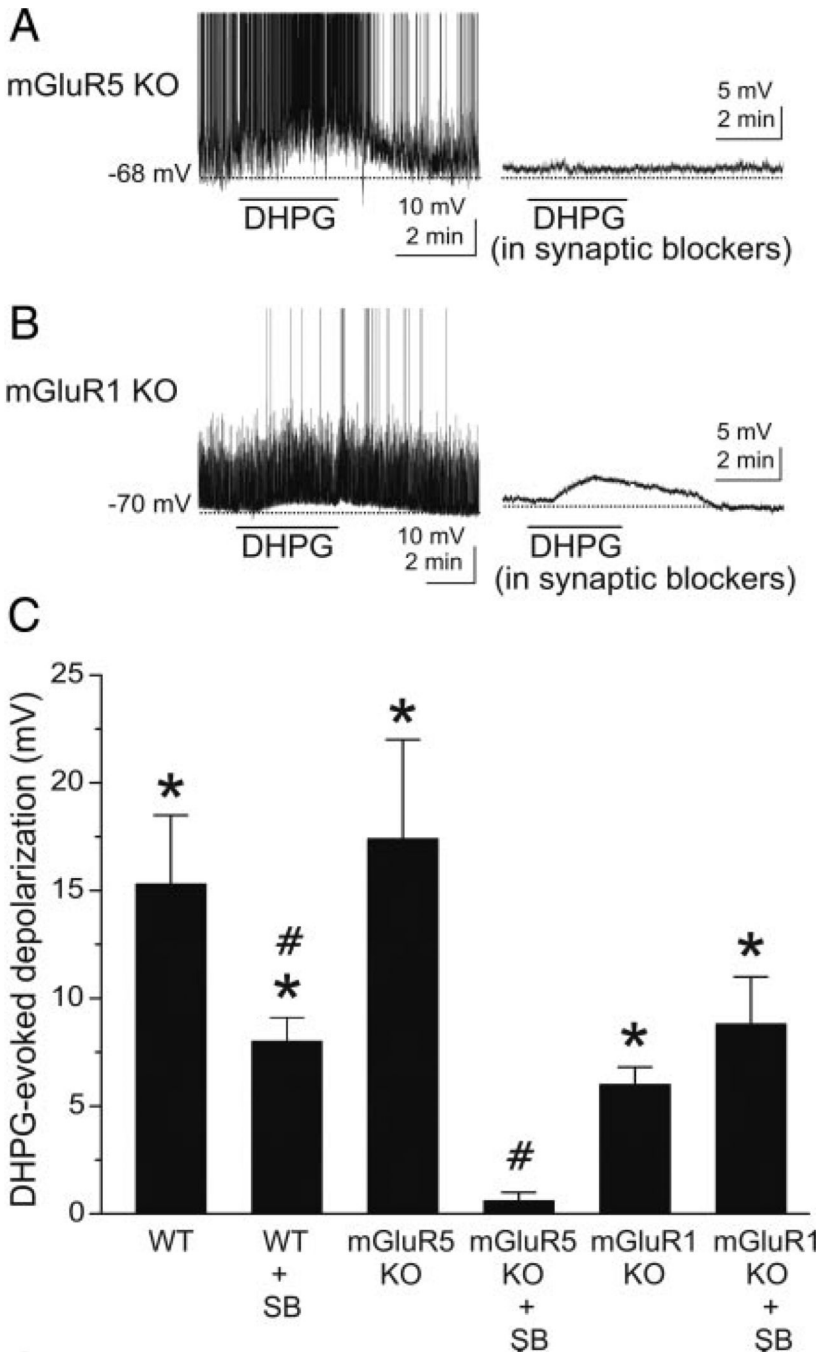

Fig. 4.

DHPG-evoked excitation of GCs is absent in mGluR5 null mutant mice. *A*, *left*: DHPG (50 μM) excites a GC recorded in a slice harvested from an mGluR5$^{-/-}$ mouse. *Right*: in the presence of synaptic blockers [CNQX (10 μM), APV (50 μM), and gabazine (5 μM)], DHPG had no effect on the same GC. *B*: in normal media (*left*), DHPG depolarizes and moderately increases the firing rate of a GC from an mGluR1$^{-/-}$ mouse. Subsequent application of DHPG (50 μM) to the same cell in the presence of synaptic blockers (*right*) elicited a comparable depolarization although evoked spikes are absent. Note that application of synaptic blockers (*right*)in *A* and *B* decreases baseline noise compared with *left control traces*, which include spontaneous EPSPs. *C*: bar graph showing group data on the effects of DHPG in wild-type and

mGluR KO mice with or without synaptic blockers present; data are expressed as DHPG-evoked depolarization (mV) compared with control. WT, wild-type mice; mGluR5 KO, mGluR5 knockout mice; mGluR1 KO, mGluR1 knockout mice; SB, synaptic blockers; see text for numbers of GCs tested. *, significantly different from control, $P < 0.05$, paired *t*-test. #, significantly different from respective non-SB group, $P < 0.05$, independent *t*-test. See text for specific *P* values. The DHPG-evoked depolarization in the mGluR1 KO group was significantly less than in the WT group ($P < 0.02$). There were no significant differences ($P > 0.05$, see text for specific *P* values) between the *1*) WT and mGluR5 KO groups, *2*) WT + SB and mGluR1 KO + SB groups, and *3*) mGluR1 KO and mGluR1 KO + SB groups.

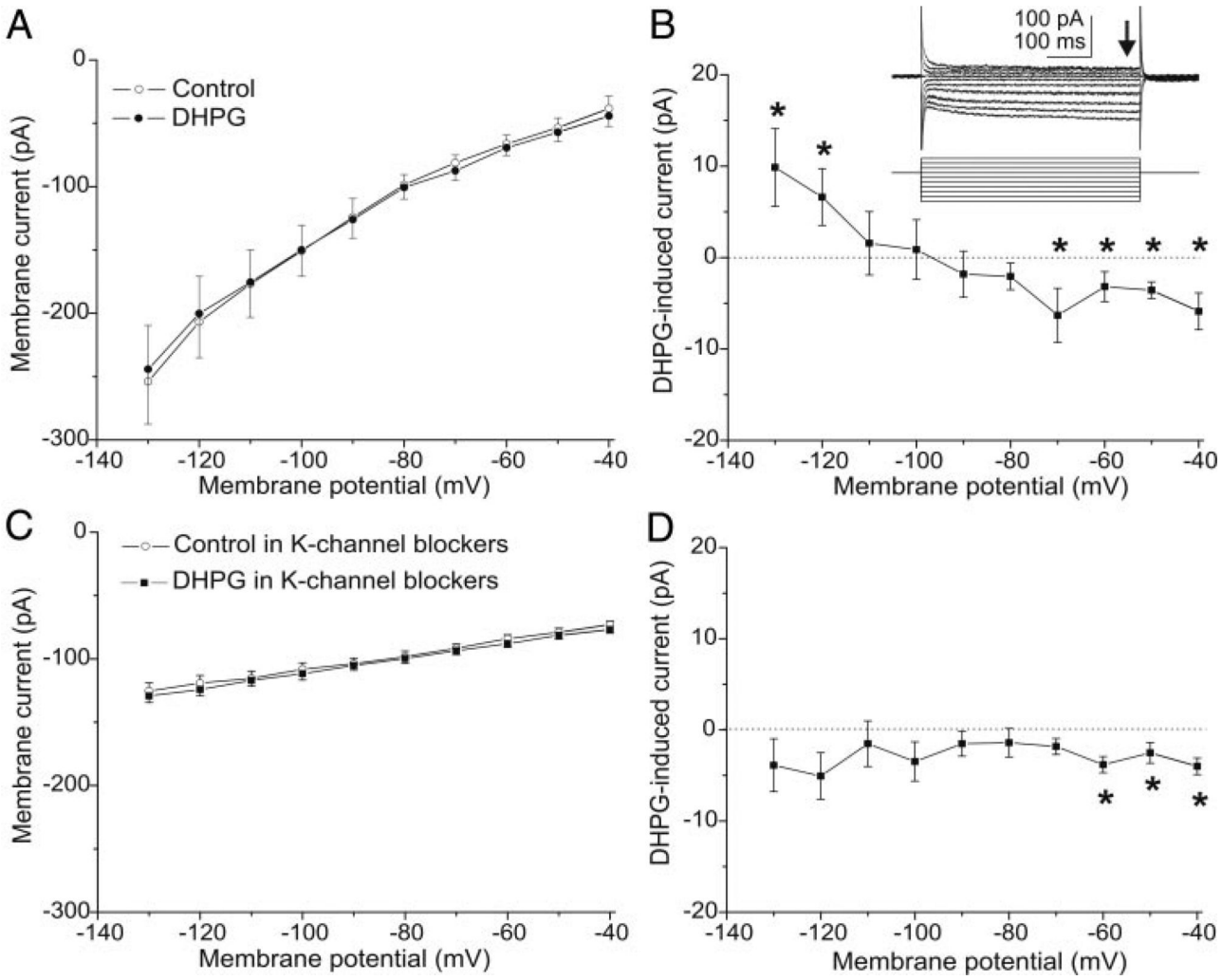

Fig. 5.

DHPG evokes an inward current in GCs. Currents elicited by 10-mV voltage steps (500 ms, V_{hold} = –70 mV) from –130 to –40 mV were recorded before and during DHPG application. Experiments in *A*–*D* were performed with blockers of fast synaptic transmission [CNQX (10 μM), APV (50 μM), gabazine (5 μM)] and TTX (1 μM) in the bath. *A*: current-voltage (*I*-*V*) curves generated under control conditions (○) and during bath application of DHPG (50 μM, •); plots represent group data from 8 mouse GCs. *B*: DHPG-induced inward current obtained by subtracting the 2 *I*-*V* curves in *A* reversed polarity close to –100 mV, near the estimated potassium equilibrium potential (–96 mV). *, values that are significantly different between the 2 curves in *A*. *Inset*: voltage steps and corresponding currents in the DHPG condition in *A*; ↓, steady-state currents used to plot *I*-*V* curves. *C*: *I*-*V* curves generated with potassium channel blockers in the bath (300 μM $BaCl_2$, 100 μM 4-aminopyridine, 20 mM TEA, 5 mM CsCl) before (○) and during (•) DHPG application; plots show group data from 6 GCs. *D*: with potassium channel blockers in the bath the DHPG current was eliminated at hyperpolarized membrane potentials. *, values that are significantly different between the 2 curves in *C*.

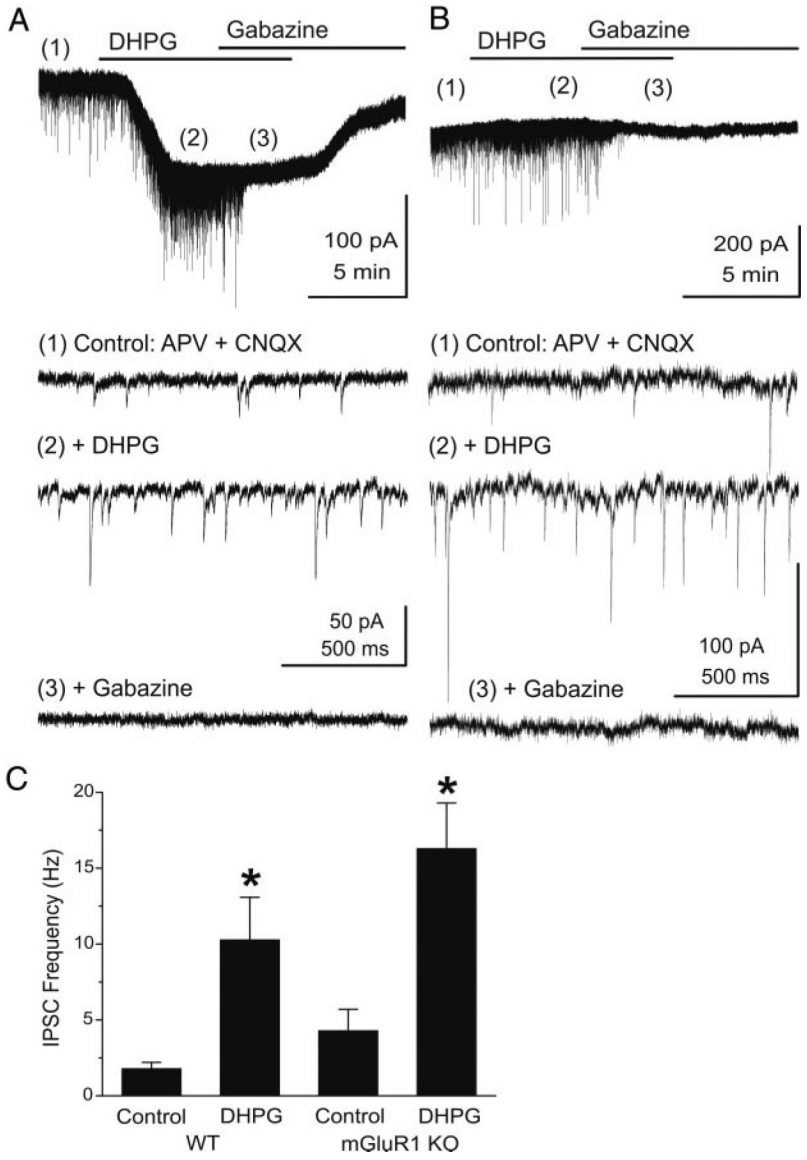

Fig. 6.

DHPG increases the frequency of GABAergic inhibitory postsynaptic currents (IPSCs) in mitral cells. Voltage-clamp recordings from mouse mitral cells were made with pipettes with a high chloride concentration (see METHODS). Ionotropic glutamate receptors were blocked with CNQX (10 μM) and APV (50 μM). Under these conditions, chloride-mediated IPSCs are reversed in polarity and appear as downward deflections (inward currents). *A, top*: application of DHPG (50 μM) evoked a prominent slow inward current in mitral cells recorded in slices from wild-type mice. Time points 1–3 are shown at faster time scale in the *3 lower traces*, respectively. Note the increase in frequency of fast IPSCs (*trace 2*), which are completely blocked by the $GABA_A$ receptor antagonist gabazine (5 μM, *trace 3*). *B*: in a mitral cell from an $mGluR1^{-/-}$ mouse, the DHPG-evoked slow inward current was absent, but DHPG substantially increased the frequency of IPSCs. Recording conditions and labeling as in *A*. *C*: bar graph summarizing the effects of DHPG on the frequency of spontaneous IPSCs in mitral cells from wild-type (WT, $n = 8$) and $mGluR1^{-/-}$ (mGluR1 KO, $n = 6$) mice. *, significantly different from respective control group, $P < 0.05$, paired *t*-test).

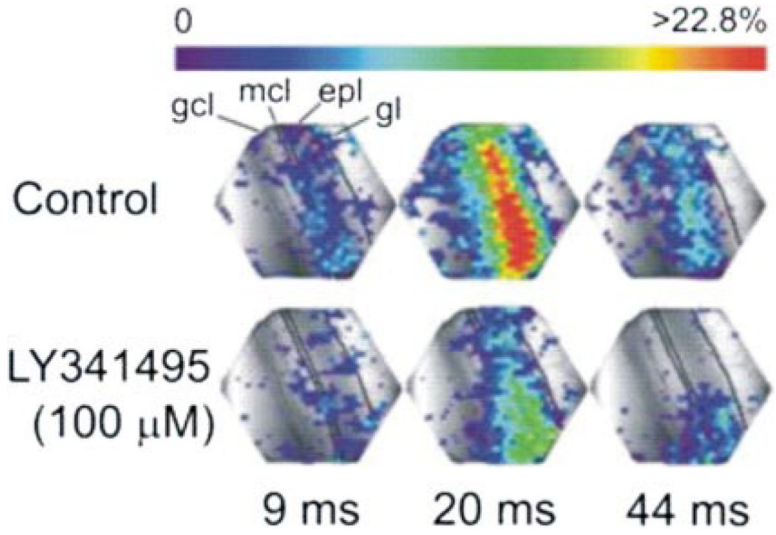

Fig. 7.

LY341495 attenuates lateral olfactory tract (LOT)-evoked optical signals. Each panel depicts the amplitude of optical responses, recorded by each of the 464 photodiodes. Signal amplitudes, expressed as a percentage above mean baseline values, are color-coded; color scale at top applies to all images. Time intervals beneath the images are relative to the onset of LOT stimulation. Single shocks applied to the LOT-elicited responses that were first observed in the external plexiform layer. LOT-evoked responses then spread sequentially into the superficial GC layer (GCL). Application of LY341495 (100 μM) reduced the amplitude of LOT-evoked voltage-sensitive dye optical signals. Gl, glomerular layer; epl, external plexiform layer; mcl, mitral cell layer.

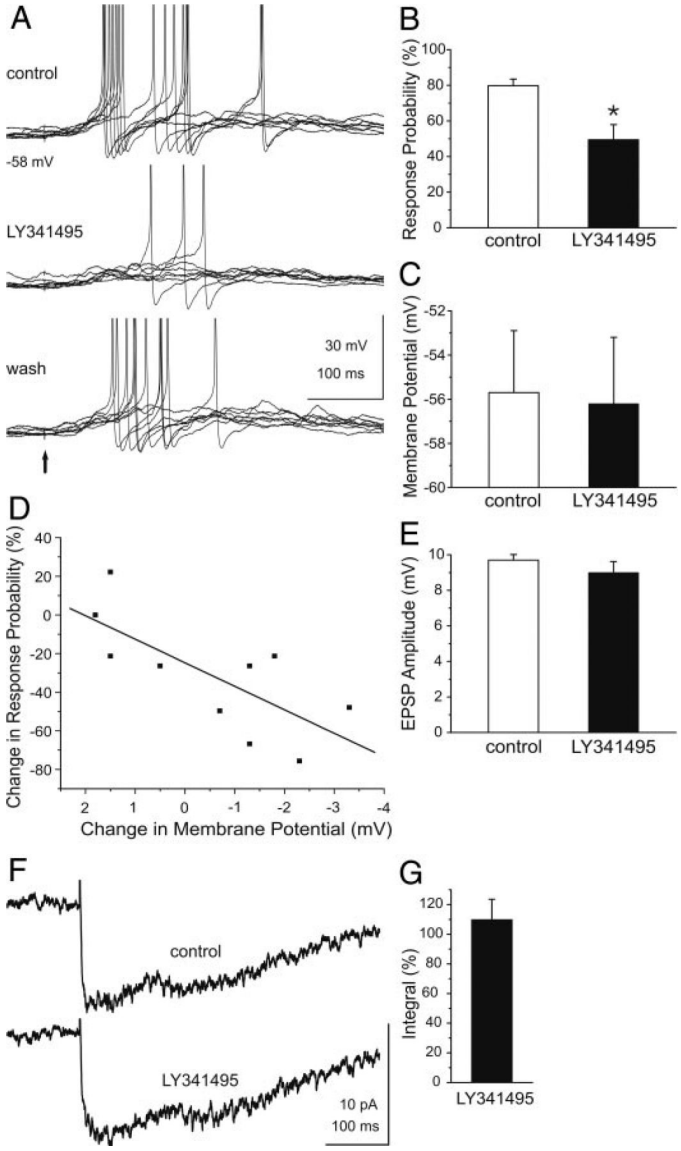

Fig. 8.

Blockade of mGluRs attenuates mitral/tufted cell-evoked excitation of GCs. *A*, *top*: single shocks (marked by ↑) applied to the glomerular layer to directly activate mitral/tufted cells evoked EPSPs and spikes in a mouse GC. *Middle*: application of LY341495 (100 μM) markedly reduced evoked excitation of the same GC in a reversible manner (*bottom*). Twelve stimulus trials are shown in each trace. *B*: bar graphs of group data (n = 10) show the percentage of glomerular layer-evoked spikes before (control) and during application of LY341495. *C*: LY341495 did not significantly alter the resting membrane potential in the group of 10 cells tested. *D*: regression analysis (see text for details) revealed that the reduction of evoked spikes in individual GCs varied with the degree of hyperpolarization. Data are fitted with a regression line (r = –0.73; P = 0.01). *E*: LY341495 did not alter the mean amplitude of the EPSP (n = 10 cells). *F*: averaged EPSC response (n = 10) to glomerular layer-evoked stimulation before (control) and during application of LY341495. *G*: bar graph of group data showing the effect of LY341495 (100 μM) on the integral of the glomerular layer-evoked EPSCs (n = 10). Data are plotted as the percentage of the control integral. LY341495 did not alter the integral of the evoked EPSCs (P < 0.45).

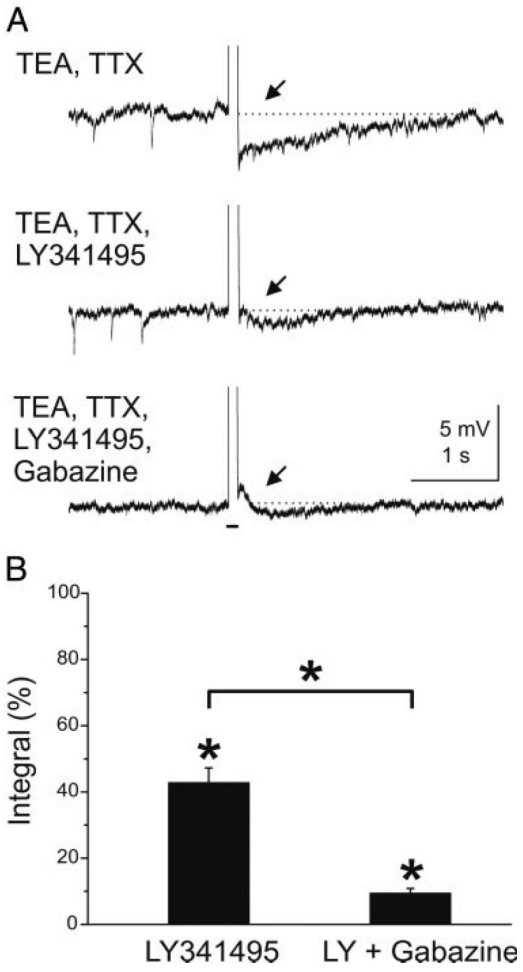

Fig. 9.

Blockade of mGluRs reduces GC-mediated feedback inhibition of mouse mitral cells. *A*: in the presence of TEA (5 mM) and TTX (1 μM) a depolarizing current pulse (100 ms, 300 pA, indicated by bar beneath *bottom trace*) applied to a mitral cell evokes a GC-mediated feedback IPSP (at ↑). Spontaneous IPSPs are visible. The feedback IPSP was reduced in amplitude and duration during bath application of the mGluR antagonist LY341495 (100 μM) (*middle*). Addition of the $GABA_A$ receptor blocker gabazine (10 μM) nearly completely abolished the remaining evoked IPSP as well as spontaneous IPSPs. *B*: bar graphs of group data showing the effect of LY341495 (100 μM) on the integral of the GC-mediated feedback IPSP ($n = 4$). Data are plotted as the percentage of the control integral in TEA and TTX. LY341495 reduced the integral of the evoked IPSPs substantially ($P < 0.000001$). Addition of gabazine further reduced the IPSP compared with LY341495 ($P < 0.000001$).